

## **Preparation Electroanalysis Based on Sensor Nanosheets G-C<sub>3</sub>N<sub>4</sub>/CPE for Determination of Amount Hg<sup>2+</sup> ion in Water Samples by Square Wave Anodic Stripping Voltammetry (SWASV) Method**

**Shahnaz Davoudi\*, Mohammad Reza Asghari Ganjeh**

*Department of Chemistry, Omidiyeh Branch, Islamic Azad University, Omidiyeh, Iran*

*(Received 14 Jun. 2021; Final revised received 18 Sep. 2021)*

### **Abstract**

This study describes the construction of a new electrochemical sensor and applies it for the determination of Hg<sup>2+</sup> ion. This sensor was prepared using new nanographene on G-C<sub>3</sub>N<sub>4</sub> nanosheets. Although the other methods (gas or liquid chromatographic, electrophoresis, flow injection) for measuring Hg<sup>2+</sup> ion have advantages such as excellent accuracy and reproducibility, it has limitations such as long-time measure, high equipment cost. Here, we report the use of an electrochemical approach for analytical determination of Hg<sup>2+</sup> ion that takes 120 s. The calibration curve was linear in the range of (0.03 to 33.0 nM). The current response was linearly proportional to the Hg<sup>2+</sup> ion concentration with a R<sup>2</sup>~ 0.999. We demonstrated a sensitivity a limit of detection of (0.093 nM). Finally, Sensor nanosheets G-C<sub>3</sub>N<sub>4</sub>/CPE has been successfully applied for the determination of Hg<sup>2+</sup> ion in different kind of water samples. The method introduced to measure Hg<sup>2+</sup> ion in real samples such as water samples was used and can be used for other samples.

**Keywords:** Hg<sup>2+</sup> ion, Electrochemical, G-C<sub>3</sub>N<sub>4</sub> nanosheets, Voltammetric method.

---

\***Corresponding author:** Shahnaz Davoudi , Department of Chemistry, Omidiyeh Branch, Islamic Azad University, Omidiyeh, Iran. E-mail: sdavoudi632@gmail.com.

## **Introduction**

Large pollutants have been released into water, soil, and air environments over the past several decades. Among these pollutant heavy metals have long been recognized as a major pollutant of the environmental [1]. Mercury (Hg) is one of the notorious heavy metals on the earth's surface and extremely harmful to humans and animals, even at low concentrations [2]. The maximum contaminant limit (MPCL) is  $0.2 \mu\text{g L}^{-1}$ , even low level of  $\text{Hg}^{2+}$  ion [3], exposure to mercury or its compounds (particularly methyl mercury) can cause a series of toxicological effects such as kidney failure, brain damage, deafness, vision impairment, loss of sensation, and poor muscle coordination [4,5].

Concern over the distinct toxicity of mercury has stimulated explorations aimed at developing price-favorable, fast, and facile methods to monitor mercury in biological, industrial and food samples [6]. According the stated reasons, a simple and rapid detection of  $\text{Hg}^{2+}$  ion is important in different types of real samples. Therefore, the detection of  $\text{Hg}^{2+}$  in water environment is of great significance for the protection of human health. To meet the need of  $\text{Hg}^{2+}$  sensing, traditional analytical methods, ion atomic fluorescence spectrometry (AFS) [7], atomic absorption spectroscopy (AAS) [8], surface-enhanced Raman scattering (SERS) [9], inductively coupled plasma atomic emission spectrometry (ICP-AES) [10], Photo electrochemical spectrometry (ICP-MS) [11], and on-line coupled systems (gas chromatography or liquid chromatography coupled with AAS, AFS, or ICP-MS [12], Surface Plasmon Resonance (RRS) [13], and selective voltammetry [14,15], have been used for  $\text{Hg}^{2+}$  determination.

Most of the researchers determined  $\text{Hg}^{2+}$  by chemical compounds method. All these determinations were time-consuming and required expensive chemicals, equipment, and sample preparation. But electrochemical methods offer advantages such as ease of use, speed, economical and good accuracy have been utilized for determining materials in different matrices and during the oxidation of material the products were adsorbed at the electrode surface and causes acute poisoning of electrode surface. Voltammetry methods (ASV) to renew electrode surface can be the good candidate in solving electrode poisoning problems. In particular, they offer favorable signal-to-noise characteristics and diversity in the way of surface modification [16,17]. Attention has newly been drawn to metal nanoparticles and graphene-based Electrochemical methods for selective and delicate reorganization of target species (organic and biomolecules) in different complex matrices [18,19]. Accordingly, G- $\text{C}_3\text{N}_4$  nanosheets have very interesting features different applications in many fields of research [20,21]. Among these method have the electrochemical can techniques for the measure of  $\text{Hg}^{2+}$  ion be highlighted [22].

There is an increasing interest in development of carbon paste electrode (CPE) and modified CPE as working electrode in the voltammetric method for selective interaction between analyses and sensing layer, chemically modified matrices have been used. The applied matrices enhanced the conductivity, surface area and sensitivity of modified electrode [23]. The other advantages of CPEs, such as ease of fabrication, have a low cost flexible substrate for modification, low ohmic resistance, high sensitivity, chemical inertness, renewable surface and compatibility with different kinds of modifiers. The sensing properties of modified CPEs are widely dependent on the nature of used materials in sensing layer. In recent years, the synthesis of nanoparticles has opened new horizons in designing of advanced electrochemical systems [24]. In the present work, an attempt has been made to provide a simple and low-cost method for measuring  $\text{Hg}^{2+}$ . The methodology applied by using of G- $\text{C}_3\text{N}_4$  nanosheets and preparing modified CPE to improve the sensitivity characterize  $\text{Hg}^{2+}$ -G- $\text{C}_3\text{N}_4$  nanosheets intensity of aggregated particles, shows the aggregated structure of G- $\text{C}_3\text{N}_4$  nanosheets with of  $\text{Hg}^{2+}$  ion when they react (Figure 1). Under optimum condition, the G- $\text{C}_3\text{N}_4/\text{CPE}$  was used for individual and determination of trace amounts of  $\text{Hg}^{2+}$  ion indifferent as a water samples.

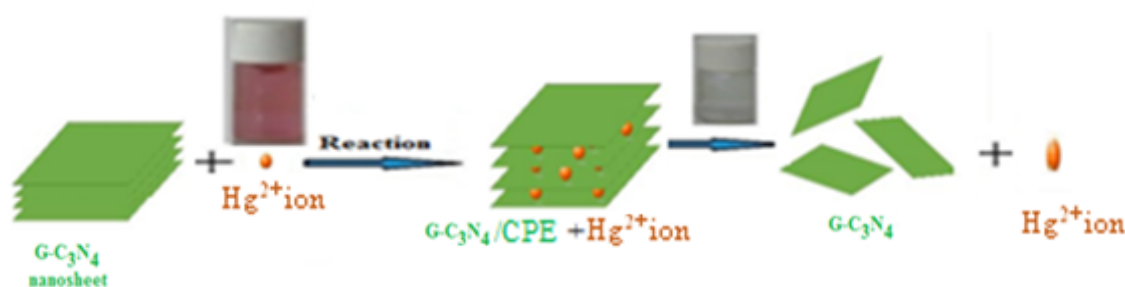


**Figure 1.** Schematic of the reaction between G- $\text{C}_3\text{N}_4$  nanosheets and  $\text{Hg}^{2+}$  ion yielding G- $\text{C}_3\text{N}_4$  nanosheets-  $\text{Hg}^{2+}$  ion complex as the product.

## Experimental

### Reagents and materials

All chemicals were provided from Merck (Darmstadt, Germany). Stock solutions of  $\text{Hg}^{2+}$  (1000 mg  $\text{L}^{-1}$ ) were prepared by dissolving appropriate amounts of  $\text{HgCl}_2$  (Merck), For  $\text{pH} < 7.0$ , as buffer solutions were prepared from 1 ml of boric acid/acetic acid/phosphoric acid (1.0 M), and for  $\text{pH} > 7.0$  was adjusted by the addition of 0.2M sodium hydroxide, DD  $\text{H}_2\text{O}$  (Double distilled water) was used in the preparation of the solutions.

### *Instrumentation*

UV–visible spectra, materials concentrations were determined and their measurements were done using a Maya Pro 180 spectrophotometer (Shimadzu Company, Japan). Potentiostat/galvanostat system (Model SAMA 500 Esfahan, Iran) and a copper wire, an Ag/AgCl/KCl (3 molL<sup>-1</sup>) were used. The structure and phase evaluation of prepared samples were characterized by Transmission electron microscopy (TEM) images which were taken on a (JEOL 3010, Hitachi Company, China). The functional groups of bulk G-C<sub>3</sub>N<sub>4</sub> were characterized by FT-IR (Nicolet Impact 400 D spectrometer) in the wave number range of 4000-400 cm<sup>-1</sup>. X- ray diffractometer (D5005, Siemens, Germany), with in the 2θ range of 10° to 80° radiation Cu-Kα, operating voltage 50 kV, operating current (tube current) 150 mA. Raman spectroscopy was performed at ambient conditions with 633 nm laser excitation (Lab RAM HR evolution, Horiba). A Genway model 3510 pH/Ion meter with a combined glass electrode was used for pH measurements.

### *Samples preparation*

Different standard amounts of Hg<sup>2+</sup> ion were spiked into 100 ml samples of Ramin power plant cooling water, Maroon dam water, Dez dam water, Karoon River water, Ahvaz drinking water and Ahvaz hospital water samples were collected in acid-leached polyethylene bottles. All water samples were collected from (Ahvaz, Iran). After standing for 24 h in refrigerator, the samples were filtered by a piece of filter paper) where the Hg<sup>2+</sup> ion content in each sample was determined blue at optimum conditions. Each test was repeated at least two times for consistency of the results. Hg<sup>2+</sup> ion content of different water samples and their recovered counterparts were subjected to further investigation. The samples were then adjusted to pH 5.5 and immediately analyzed [25].

### *Procedure synthesis sensor G-C<sub>3</sub>N<sub>4</sub> nanosheets*

G-C<sub>3</sub>N<sub>4</sub> nanosheets were facilely fabricated by thermal polymerization and then exfoliated into ultrathin nanosheets through ultrasonication in water media. Low-cost C-N nanosheets prepared by melamine possessed a highly π-conjugated structure property. Synthesis, the G-C<sub>3</sub>N<sub>4</sub> initially, 20.0 g of powder melamine was placed in the alumina in a special system and in N<sub>2</sub> gas, with the coating and then heated for 2 hours at 600°C (temperature: 3 °C in 1 min), resulting in a yellow powder (Figure 2). The bare CPE was used adopted an aqueous phase exfoliation method for the preparation of g-C<sub>3</sub>N<sub>4</sub> nanosheets. Herein, 0.05 g bulk g-C<sub>3</sub>N<sub>4</sub> was stirred for 1 hours and then ultrasonicated for in a hot water bath. The aqueous dispersed carbon nitride nanosheets formed were centrifuged at 4500 rpm. The supernatant was again centrifuged at 12000 rpm to obtain g-C<sub>3</sub>N<sub>4</sub> nanosheets [26,27].

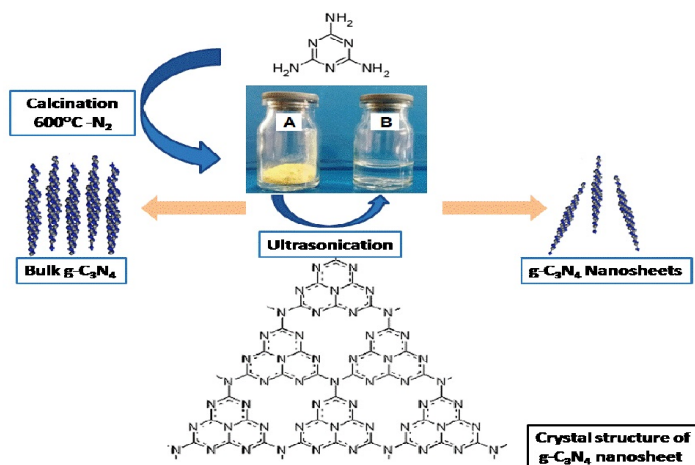


**Figure 2.** Schematic of G-C<sub>3</sub>N<sub>4</sub> nanosheet synthesis, also, this is a picture of G-C<sub>3</sub>N<sub>4</sub> (A) and the dispersion of products in water (B) obtained after G-C<sub>3</sub>N<sub>4</sub> ultrasonic treatment.

### Analytical Method

Determination of analyte of Hg<sup>2+</sup> ion by SWASV technique under optimized condition were in an 20 mL capacity cell in cloud electrolytic platinum, and buffer solution as a supporting electrolyte medium, pH 5.5, time 120 s, and solution of Hg<sup>2+</sup> was investigated at peak currents range, -0.8 to 0.2 V, Therefore, peak currents of -0.4 V reaction was chosen in this experiment.

## Results and discussion

### Characterization of synthesized G-C<sub>3</sub>N<sub>4</sub> nanosheets

The structural characteristics such as shape and size of G-C<sub>3</sub>N<sub>4</sub> nanosheets and G-C<sub>3</sub>N<sub>4</sub>-Hg<sup>2+</sup> and also aggregation phenomenon were investigated. FT-IR spectrum was recorded to determine the surface functional groups present on the prepared bulk G-C<sub>3</sub>N<sub>4</sub> in (Figure 3a) exhibits a broad band at 3292 cm<sup>-1</sup>. Which can be attributed to the stretching vibration modes of the NH<sub>2</sub> or N-H groups. The peaks at 1242 cm<sup>-1</sup>, 1325 cm<sup>-1</sup>, 1423 cm<sup>-1</sup>, 1560 cm<sup>-1</sup> and 1642 cm<sup>-1</sup> correspond to the typical stretching vibration modes of C = N and C-N heterocycles. The small peak located at 806 cm<sup>-1</sup> is a signature of the characteristic breathing vibration mode present in G-C<sub>3</sub>N<sub>4</sub> [28]. The absorption feature at 889 cm<sup>-1</sup> was associated to a deformation mode of cross-linked heptazine. Upon the addition of Hg<sup>2+</sup>, G-C<sub>3</sub>N<sub>4</sub> nanosheets aggregated due to the presence of substance with groups S and N (Fig. 3b). The XRD patterns of G-C<sub>3</sub>N<sub>4</sub> nanosheets are shown in (Figure 3b). The XRD pattern of the nanosheets G-C<sub>3</sub>N<sub>4</sub>, which is matched with the standard sample [29]. The G-C<sub>3</sub>N<sub>4</sub> nanosheets shapes are distorted spherical, with an average size range of 25-30 nm as shown by TEM image (Figure 4a). Figure 4b, shows the Raman spectrum of synthesized bulk G-C<sub>3</sub>N<sub>4</sub> with several characteristic bands observed at 1579, 1482, 1149, 985, 705 and 473 cm<sup>-1</sup> corresponding to the typical vibration modes of C-N and C=N heterocycles [30,31].

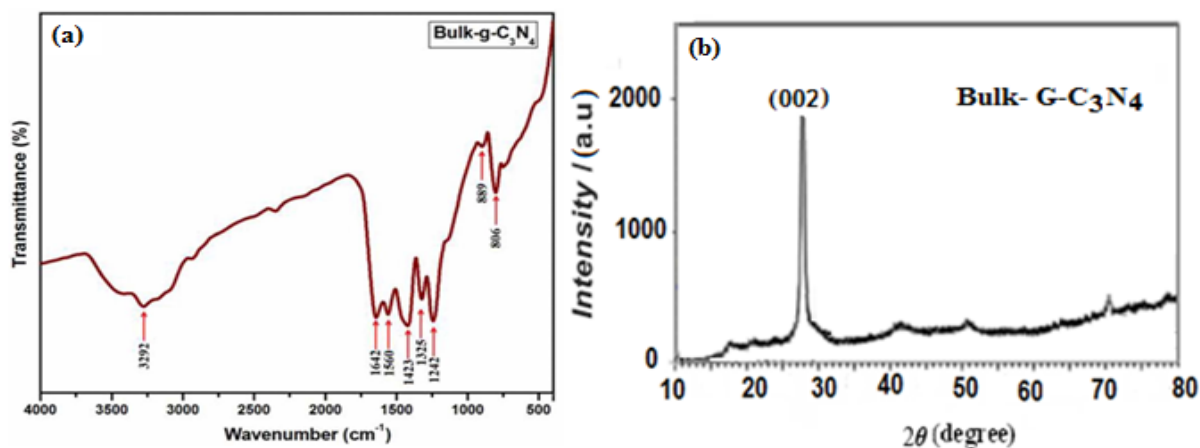


**Figure 3.** (a) FT-IR spectrum of synthesized bulk G-C<sub>3</sub>N<sub>4</sub> nanosheets. (b) XRD pattern of synthesized bulk G-C<sub>3</sub>N<sub>4</sub> nanosheets.

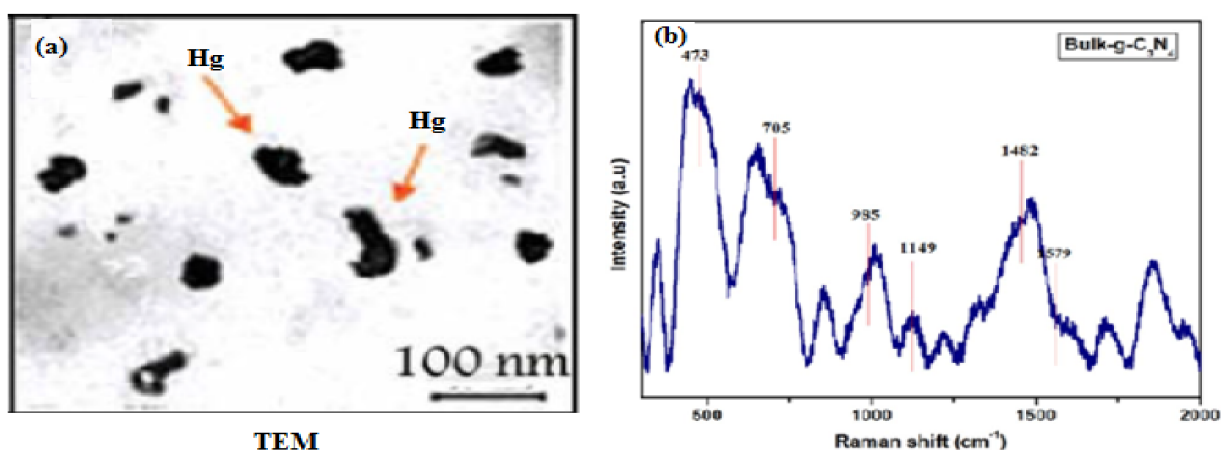


**Figure 4.** (a) TEM image of carbon nitride graphite and addition of analysis Hg<sup>2+</sup>-G-C<sub>3</sub>N<sub>4</sub> nanosheets. (b) Raman spectrum of bulk G-C<sub>3</sub>N<sub>4</sub> (with 633 nm excitation).

#### *Electrochemical oxidation of Hg<sup>2+</sup> by nanosheets G-C<sub>3</sub>N<sub>4</sub>/CPE*

Electrochemical oxidation of 10.0 nM of Hg<sup>2+</sup> was tested on a bare CPE and nanosheets G-C<sub>3</sub>N<sub>4</sub>/CPE (at a scan rate of 50 mV s<sup>-1</sup> in nanosheets G-C<sub>3</sub>N<sub>4</sub>/CPE is illustrated in (Figure 5). As Hg<sup>2+</sup> oxidation is a two-electron transfer process. Hence, the electrochemical oxidation of Hg<sup>2+</sup> on nanosheets G-C<sub>3</sub>N<sub>4</sub>/CPE takes place by direct transfer of two protons and two electrons by a chemical conversion. The impact of scan rate ( $\nu$ ) on Hg<sup>2+</sup> oxidation peak current ( $I_p$ ) was investigated at G-C<sub>3</sub>N<sub>4</sub> using by electrochemical (SWASV) measurement method (Figure 8), shows voltammograms (SWASV) of the nanosheets G-C<sub>3</sub>N<sub>4</sub>/CPE in 10.0 nM of Hg<sup>2+</sup> at different scan rates from 10 to 100 mV s<sup>-1</sup>. According to the Randles-Sevcik formula (Equation. 1), it can be clearly seen that the increases against square roots of scan rate with a linear correlation coefficient of ( $R^2$  pa Where  $I_p$ ) 0.9986 (Figure 9) [32].

$$I_p = (2.69 \times 10^5) n^{3/2} A D^{1/2} C v^{1/2} \quad (1)$$

Is the oxidation peak current (A),  $n$  is the number of transferred electrons per mole,  $A$  is the active surface area of the electrode ( $\text{cm}^2$ ),  $D$  is the diffusion coefficient ( $\text{cm}^2/\text{sec}$ ),  $C$  is concentration ( $\text{mol}/\text{cm}^3$ ) and  $v$  is the scan rate ( $\text{V}/\text{s}$ ). These results indicated that the oxidation of  $\text{Hg}^{2+}$  on nanosheets G- $\text{C}_3\text{N}_4/\text{CPE}$  is a diffusion-controlled electrochemical processes [33].

#### SW Voltammograms in the absence electrolyte and presence of $\text{Hg}^{2+}$ in bare CPE

Electrochemical measurements the scanning was from  $-0.8$  to  $0.2$  V; the amplitude was  $0.1$  V; the step height potential  $5$  mV; the time of integration was  $10$  seconds; and the frequency was  $50$  Hz. To individual detection of  $\text{Hg}^{2+}$  by electrochemical (SWASV) measurement method; this in work electrode has been modified with a G- $\text{C}_3\text{N}_4$  nanosheets by putting it into a solution including in phosphate buffer (pH 5.5). As shown in (Figure 5), was obtained potential  $-0.4$  V for determination of  $\text{Hg}^{2+}$  in solution [34,35].

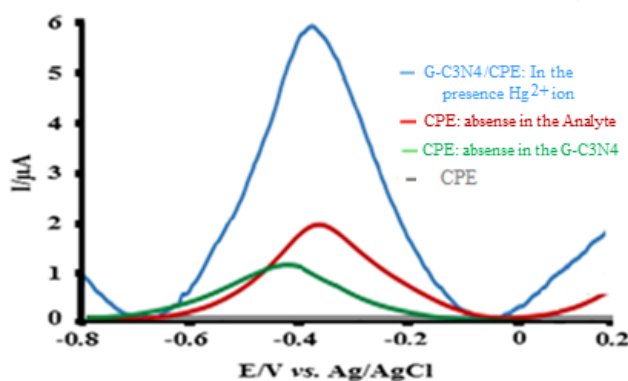


**Figure 5.** SW voltammograms in the absence electrolyte and presence  $10.0$  nM of  $\text{Hg}^{2+}$  ion in electrochemical conditions on the surface of bare CPE: (line blue) absence by G- $\text{C}_3\text{N}_4$  in the presence  $\text{Hg}^{2+}$  ion, (line red) absence CPE of the analyte and (line green) absence G- $\text{C}_3\text{N}_4$  nanosheets/CPE.

#### Optimization of Sensing Conditions parameters on the voltammetric current

Obtaining an exceptionally sensitive response in detecting  $\text{Hg}^{2+}$  rests upon the systematic optimization of pH values, nanosheets G- $\text{C}_3\text{N}_4$  and incubation time.

#### Electrochemical behavior of $\text{Hg}^{2+}$ ion at the screen-printed carbon electrode

The electrochemical response of  $\text{Hg}^{2+}$  ion was measured against the background solution to investigate if the observed signal was due to the  $\text{Hg}^{2+}$  ion that there is no response from the background and a very clear signal appearing for the  $\text{Hg}^{2+}$  ion at a potential around  $-0.4$  V [36].

### Effect of pH

The effect of pH on the current responses of 10.0 nM of  $\text{Hg}^{2+}$  ion on the nanosheets G- $\text{C}_3\text{N}_4/\text{CPE}$  was investigated in the range of 2.0 to 7.0 by SWV. The stripping current for the analyte have been raised by increasing of pH up to 5.5, as shown in (Figure 6). The peak current was decreased by further increasing of pH, it may be owing to the  $\text{Hg}^{2+}$  ion hydrolysis. Hence, the pH of 5.5 was selected for subsequent experiment [37].

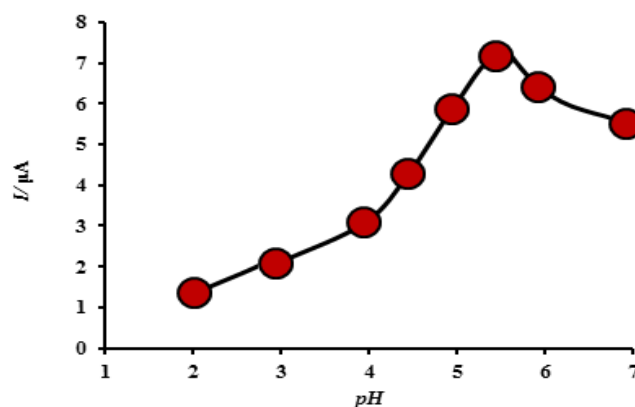


**Figure 6.** Impact of pH on the on the voltammetric current for 10.0 nM of  $\text{Hg}^{2+}$  ion in phosphate buffer solution.

### Effect of buffer

In this section, the best type of buffer and its volume for maximum of  $\text{Hg}^{2+}$  ion availability for detection purpose with nanosheets G- $\text{C}_3\text{N}_4/\text{CPE}$  sensor are investigated. In order to choose the optimal buffer, three buffers (citrate, acetate and phosphate buffer) were investigated that phosphate buffer was the best. Furthermore, 1.0 mL of (0.1 M) phosphate buffer as a supporting electrolyte medium in different concentrations of  $\text{Hg}^{2+}$  ion was selected as optimum.

### The effect of deposition time

The effect of deposition time on the stripping responses of  $\text{Hg}^{2+}$  ion was studied from 25 to 150 s with a deposition potential of  $-0.4$  V, and it has been found that the oxidation response increased by increasing the accumulation time up to 120 s. This is owing to the fact that the longer collection time caused more  $\text{Hg}^{2+}$  ion to get accumulated at the electrode/solution interface onto modified surface. It can be seen that after 120 s, the stripping currents become approximately constant owing to surface saturation [38]. Hence, the accumulation time of 120 s was chosen in this experiment as shown in (Figure 7).

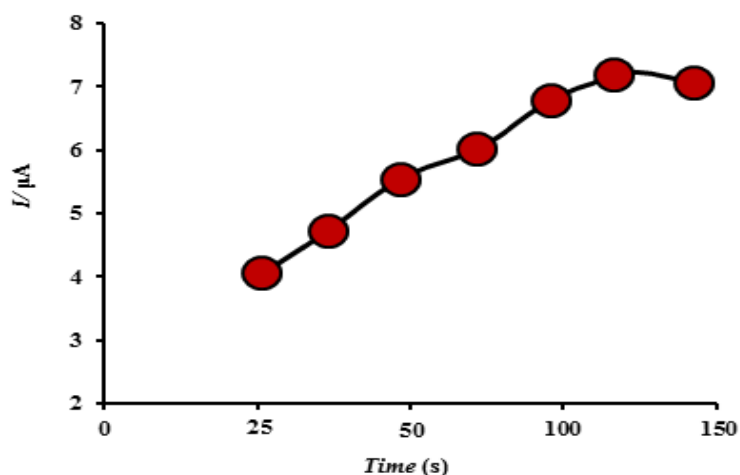


**Figure 7.** Impact of deposition time on the voltammetric current for 10.0 nM of  $\text{Hg}^{2+}$  ion in pH 5.5 in phosphate buffer solution.

### Calibration curve

The excellent electrocatalytic activity of the nanosheets  $\text{G-C}_3\text{N}_4/\text{CPE}$  electrode, which was examined in the previous sections, makes it possible to measure  $\text{Hg}^{2+}$  ion at low concentrations. For this purpose and for the analysis of solutions, first it is necessary to prepare a calibration curve to use it to measure the concentration of unknown samples [39]. To prepare the calibration curve, solutions with different concentrations of  $\text{Hg}^{2+}$  ion (from 0.03 to 33.0 nM) were prepared and their voltamogram was obtained using the (SWASV) technique, which is shown in (Figure 8). It can be seen that as the concentration of  $\text{Hg}^{2+}$  ion gradually increases, its peak oxidation current also increases and there is a direct and linear relationship between the concentration and the peak oxidation current, which is calibration equation the  $\text{Hg}^{2+}$  ion, shown in (Figure 9). The precision of the method was evaluated by performing (n=10) replicate measurements of  $\text{Hg}^{2+}$  ion solutions. The Relative Standard Deviations (RSD) for these determinations was (2.3 %), and Limit of Detection (LOD) ( $0.093 \mu\text{g L}^{-1}$ ) respectively (Figure 9) [40,41].

$$I_{pa} = 0.4988C_{\text{Hg}} + 0.319 \quad (R^2=0.9986).$$

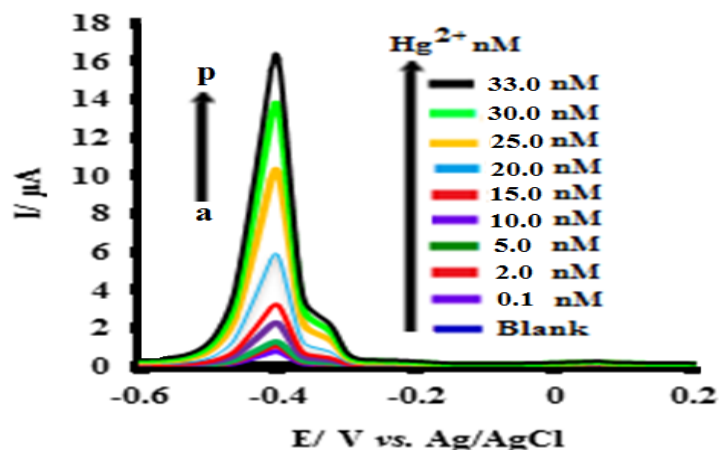


**Figure 8.** SWASV voltammograms using  $C_{\text{Hg}}$  the analytes concentrations. nanosheets G- $\text{C}_3\text{N}_4/\text{CPE}$  for  $\text{Hg}^{2+}$  ion (0.03–33.0 nM) under optimum condition.

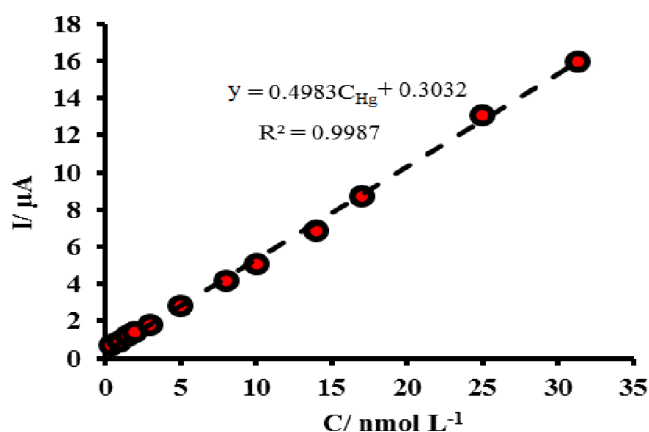


**Figure 9.** Calibration plot of the voltammetric currents as a function of the analytes concentrations.

#### *Evaluation of reproducibility and stability of the modified electrode*

Nanosheets G- $\text{C}_3\text{N}_4/\text{CPE}$  electrode reproducibility by recording Square wave anodic stripping voltammetry (SWASV) (repeated)  $n=10$  (from constant concentrations of  $\text{Hg}^{2+}$  ion) 10.0 nM (at pH 5.5 and extracting peak currents from each voltammogram were studied. The relative standard deviation (RSD) was calculated to be 2.3%, which indicates the excellent reproducibility of the modified electrode results and the high accuracy of the introduced analytical method. Also, the stability of the electrode by polishing the electrode surface and 10.0 nM of  $\text{Hg}^{2+}$  ion voltammogram was recorded at pH = 5.5 and then the electrode was stored for two weeks in ambient conditions and the voltammogram was recorded and compared with the initial voltammogram. It was found that the peak currents were equal after two weeks. 98% were their initial values. This test was performed on the electrode again after one month and two months and the obtained currents had reached 95.2% and 95.6% of their initial values, respectively, which indicates the good stability of the electrode and a long shelf life. The results indicate that the G- $\text{C}_3\text{N}_4$  nanosheets/CPE retained 95.0%

of its initial stripping response after a period of 14 days, has excellent repeatability, reproducibility, and long-term stability [42].

#### *Optimum values of parameters*

The optimum values of parameters are demonstrated in Table.1. The method can be used as an alternative method for Hg<sup>2+</sup> ion measurement owing to advantages like excellent selectivity and sensitivity, low cost, simplicity, low detection limit and no need in utilizing organic harmful solvent.

**Table 1.** Investigation of method repeatability at conditions.

Parameter	Optimum Value for Hg <sup>2+</sup> ion
Hg <sup>2+</sup> ion	(10.0 nM)
pH	5.5
Equilibration time (s)	(120 s)
Linear range (LDR)	(0.03 – 33.0 µgL <sup>-1</sup> )
Detection limit (LOD)	(0.093 nM)
Relative Standard Deviations (RSD)	(2.3%)
Advantages	High repeatability, sensitivity, selectivity, wide linear range and no need to organic solvent

#### *Interference Studies*

The electro active compounds that are present in the real samples might be a potential interference during the electrochemical determination of the analytes. Among what we studied were also the interaction between anions and cations on Hg<sup>2+</sup> ion direction. To perform these studies, various ions were introduced into the solution that contained 10.0 nM of Hg<sup>2+</sup> ion and then applying the general procedure [14,43]. As exhibited in (Table 2), the tolerance limit was determined as the maximum concentration of the interfering substance which resulted in an error less than (±5%) for determination of Hg<sup>2+</sup> ion. The So selectivity of the recommended method was proven.

**Table 2.** Limit of tolerance foreign ions on determination of Hg<sup>2+</sup> ion (n=6).

Foreign species	Tolerance limit (nM)
NH <sub>4</sub> <sup>+</sup> , Mg <sup>2+</sup> , Na <sup>+</sup> , K <sup>+</sup> , Ca <sup>2+</sup>	1000
CO <sub>3</sub> <sup>2-</sup> , SO <sub>4</sub> <sup>2-</sup> , Cl <sup>-</sup> , I <sup>-</sup>	1000
Cr <sup>3+</sup>	250
Ag <sup>+</sup> , Fe <sup>2+</sup> , Fe <sup>3+</sup>	100

#### *Analysis of water samples*

Several tests were carried out in order to determination of Hg<sup>2+</sup> ion in different real samples. As it can be seen in Table 3, the results of the measurements are comprised to those obtained by Square wave anodic stripping voltammetry (SWASV) method which confirmed the accuracy and reliability of the method [44,45]. Hence the proposed method can be used for individual and simultaneous

detection of  $\text{Hg}^{2+}$  ion in different real samples. The obtained percentage percentiles in (Table.3), indicate that the prepared G- $\text{C}_3\text{N}_4$  nanosheets/CPE sensor has a very good performance for determination of  $\text{Hg}^{2+}$  ion in water samples.

**Table 3.** Analytical results of the determination of  $\text{Hg}^{2+}$  ion content and recovery test of  $\text{Hg}^{2+}$  ion in water samples with the proposed method (n=5).

Samples	Added ( $\mu\text{g mL}^{-1}$ )	Founded ( $\mu\text{g mL}^{-1}$ )	RSD %	Recovery %
Hospital Ahvaz	0.00	0.32	2.6	----
River water	0.10	1.34	1.5	98.9
Ramin power plant	0.00	0.51	3.6	----
cooling water	0.10	1.54	2.3	101.6
Karon River waverAhvaz	0.00	0.93	1.1	----
	0.10	1.94	0.9	103.4
Dez dam water	0.00	0.83	3.9	----
	0.10	1.85	2.3	104.0
Maroon dam water	0.00	0.46	2.9	----
	0.10	1.44	1.8	102.0

#### Comparison of this method with other methods

A comparison of the proposed method with the other previously reported methods demonstrates the feasibility of SWASV method and its reliability for the analysis of  $\text{Hg}^{2+}$  ions (Table. 4). The LOD and LDR in this work are comparable with and lower than some studies. RSD is better than some and comparable with those of the other studies. It can be concluded that SWASV is a sensitive method that can be used for the ultra preconcentration and extraction of  $\text{Hg}^{2+}$  ions from environmental samples.

**Table 4.** Comparisons of proposed method with other grapheme – based  $\text{Hg}^{2+}$  ion sensor.

Sensing platform / Method	LOD (nM)	Working Range (LDR)	Detection time	References
NiS-rGO - SWASV	0.8 nM	0.1-110 nM	20 min	22
SsDNA-NanoAu-G - SWV	1.0 nM	1.0 -100 nM	60 min	24
Nafion/cys-Au@Ag BMNps/GCE DPV	0.1 nM	0.1 -100 $\mu\text{M}$	300 sec	35
$\text{Co}_3\text{O}_4$ - $\text{CeO}_2$ - $\text{ZnO}$ - SWASV	0.44 nM	0.03-33 $\mu\text{M}$	120 min	40
Hydroxyapatite (HA) nanoparticles modified GCE SWA	1.41 nM	0.2-210 $\mu\text{M}$	240 sec	43
G- $\text{C}_3\text{N}_4$ nanosheets - SWASV	0.093 nM	0.03-33 $\mu\text{M}$	120 sec	This work

#### Conclusion

This study provides a new modified carbon paste electrode based on G- $\text{C}_3\text{N}_4$  nanosheets for determination of  $\text{Hg}^{2+}$  ion in Ramin power plant cooling water, Maroon dam water, Dez dam water, Karon River water, Ahvaz drinking water and hospital Ahvaz water. The obtained results suggest

that nanosheets G-C<sub>3</sub>N<sub>4</sub> is better than some other modifier of CPE for the electrochemical determination of Hg<sup>2+</sup> ion. On the other hand, some of advantages for this work are listed below:

- (I) The fabricated electrochemical sensor showed good anti-interference, stability and repeatability.
- (II) Which greatly promoted its potential usage in high-performance electrochemical sensors for the individual and simultaneous detection of toxic materials.
- (III) The results showed the studied method would be a promising method to use in routine analytical applications.

### Acknowledgements

The authors gratefully acknowledge the supports to this work by the Islamic Azad University, Omidyeh Branch, Iran.

### References

- [1] L.R.P. Mandoc, I. Moldoveanu, R.I. Stefan-van Staden, E.M. Ungureanu, *Microsystem. Technol.*, 23(5), 1141 (2017).
- [2] S. Sobhanardakani, R. Zandipak, *J. Clean. Techn. Environ. Policy.*, 19(7), 1913 (2017).
- [3] X. Guo, B. Du, Q. Wei, J. Yang, L. Yan, W. Xu, *J. Hazar. Meter.*, 278, 211 (2014).
- [4] M. Ramalingam, V.K. Ponnusamy, *J. Microchim. Acta.*, 186, 1 (2019).
- [5] Y. Zhang, L. Zhang, B. Han, P. Gao, Q. Wu, A. Zhang, *Sensors & Actuators: B. Chemical.*, 272, 331 (2018).
- [6] B. Babamiri, A. Salimi, R. Hallaj, *Biosens. Bioelectron.*, 102, 328 (2018).
- [7] S. Prabu, S. Mohamad, *J. Mol. Structure.*, (2020). Doi:Org/10.1016/j.molstruc. 2019.127528.
- [8] N. Bansal, J. Vaughan, A. Boullemant, *J. Microchem.*, 113, 36 (2014).
- [9] Y. Tian, H.F. Wang, L.Q. Yan, X.F. Zhang, A. Falak, P.P. Chen, F.L. Dong, L.F. Sun, W.G. Chu, *Chinese. Physics. B.*, 27, 77406 (2018).
- [10] G. Jarzynska, J. Falandysz, *J. Environ. Eng.*, 46(6), 569 (2011).
- [11] G. Wen, X. Wen, M.M.F. Choi, *Sensors and Actuators B-Chemical*, 221, 1449 (2015).
- [12] S.S. de Souza, A.D. Campiglia, F. Barbosa, *J. Analytica. Chimica. Acta*, 761, 11 (2013).
- [13] Z. De Liu, Y. F. Li, J. Ling, C. Z. Huang, *Environ. Sci. Technol.*, 43(13), 5022 (2009).
- [14] Q. Zhao, Y. Chai, R. Yuan, J. Luo, *Sens. Actuators B-Chem.*, 178, 379 (2013).
- [15] N. Zhou, H. Chen, J. Li, L. Chen, *Microchimica Acta*, 180, 493 (2013).
- [16] S. Davoudi, M.H. Givianrad, *Russian Journal of Electrochemistry*, 56, 506 (2020).

- [17] B. Chen, Z. Huang, X. Chen, Y. Zhao, Q. Xu, S. Chen, X. Xu, P. Long, *Electrochim. Acta*, 210, 905 (2016).
- [18] N. Nunez-Dallos, M.A. Macias, O. Garcia-Beltran, J.A. Calderon, E. Nagles, *J. Electroanal. Chem.*, 822, 95 (2018).
- [19] F. Bai, H. Huang, Y. Tan, Ch. Hou, P. Zhang, *Electrochim. Acta*, 176, 280 (2015).
- [20] H. Beitollahi, S.Z. Mohammadi, M. Safaei, S. Tajik, *Anal. Methods.*, 12, 1547 (2020).
- [21] H. Bagheri, A. Shirzadmehr, M. Rezaei, H. Khoshsafar, *Ionics.*, 24, 833 (2018).
- [22] T.D. Vu, P.K. Duy, H.T. Bui, S.H. Han, H. Chung, *Sensors and Actuators Chemical. B.*, 281, 320 (2019).
- [23] H. Bagheri, A. Afkhami, H. Khoshsafar, *Anal. Chim. Acta*, 870, 56 (2015).
- [24] Y. Zhang, G.M. Zeng, L. Tang, J. Chen, Y. Zhu, Y. He, *Anal. Chem.*, 87, 989 (2015).
- [25] H. Shafiekhani, F. Nezam, Sh. Bahar, *J. Serb. Chem. Soc.*, 82(3), 317 (2017).
- [26] A. Hatamie, F. Marahel, A. Sharifat, *Talanta*, 176, 518 (2018).
- [27] X. Yu, Z. Liu, Y. Wang, H. Luo, X. Tang, *New. J. Chem.*, 44, 15908 (2020).
- [28] M.H. Vu, C.C. Nguyen, T.O. Do, *Chem. Photo. Chem.*, 5(5), 466 (2021).
- [29] J. Hong, J. Kim, R. Selvaraj, Y. Kim, *Toxicol. Environ. Chem.*, 103(3), 18 (2021).
- [30] C. Prasad, H. Tang, I. Bahadur, *J. Mol. Liquid.*, 281, 634 (2019).
- [31] N. Murugan, M.B. Chan-Park, A.K. Sundramoorthy, *J. Electrochem. Soc. B.*, 166, 3163 (2019).
- [32] N. Tukimin, J. Abdullah, Y. Sulaiman, *J. Electrochemical Soc.*, 165, B258 (2018).
- [33] S. Huang, S. Song, H. Yue, X. Gao, B. Wang, E. Guo, *Sensors and Actuators B: Chem.*, 277, 381 (2018).
- [34] M.A. Karimi, V. H. Aghaei, A. Nezhadali, N. Ajami, *Food. Anal. Methods*, 11(10), 2907 (2018).
- [35] S. Siddiqui, A. Nafady, H.M. El-Sagher, S.I. Al-Saeedi, A.M. Alsalmeh, F.N. Talpur, S.T.H. Sherazi, M.S. Kalhor, M.R. Shah, S.T. Shaikh, M. Arain, S.K. Bhargava, *J. Solid. State. Electrochem.*, 23, 2073 (2019).
- [36] J. Penagos-Llanos, O. Garcia-Beltran, J.A. Calderon, J.J. Hurtado-Murillo, E.J. Nagles, *Electroanal. Chem.*, 852, 113517 (2019).
- [37] H. Rajabi, M. Noroozifar, M. Khorasani-Motlagh, *J. Anal. Bioanal. Electrochem.*, 8, 522 (2016).
- [38] H. Xie, Y. Niu, Y. Deng, H. Cheng, G. Li, W. Sun, *J. Chin. Chem. Soc.*, 61, 1 (2020).
- [39] T. Rahmani, A. Hajian, A. Afkhami, H. Bagheri, *New. J. Chem.*, 42(9), 7213 (2018).

- [40] S. Davoudi, M.H. Givianrad, M. Saber-Tehrani, P. Aberoomand Azar, *Ind. J. Chem.*, 58, 1075 (2019).
- [41] S.S. Hassan Sirajuddin, A.R. Solangi, T.G. Kazi, M.S. Kalhor, Y. Junejo, Z.A. Tagar, N.H. Kalwar, *J. Electroanal. Chem.*, 682, 77 (2012).
- [42] A.C. Lokhande, N.M. Shinde, A. Shelke, P.T. Babar, J.H. Kim, *J. Solid. State. Electrochem.*, 21(9), 2747 (2017).
- [43] L. Laffont, T. Hezard, P. Gros, L.E. Heimbürger, J.E. Sonke, P. Behra, D. Evrard, *Talanta*, 141, 26 (2015).
- [44] P.A. Kolozof, A.B. Florou, K. Spyrou, J. Hrbac, M.I. Prodromid, *Sensor. Actuat. B-Chem.*, 304, 127268 (2020).
- [45] K. Nagaraj, P. Senthil Murugan, S. Thangamuniyandi, *Arabian Journal of Chemistry*, 12(8), 1945 (2019).